J. Am. Chem. Soc. **1995,** *117,* 12218–12226

Organotransition-Metal Metallacarboranes. 43. Directed Synthesis of Carborane-Endcapped Multidecker Sandwiches[1,2]

Xiaotai Wang, Michal Sabat, and Russell N. Grimes*

Contribution from the Department of Chemistry, University of Virginia, Charlottesville, Virginia 22901

Received August 11, 1995[⊗]

Abstract: Triple-decker and tetradecker sandwich complexes having planar C_2B_3 or pyramidal C_2B_4 carborane ligands at one or both ends, the first examples of this genre, were prepared and characterized. A 3-way reaction of the Cp*Co(2,3-$Et_2C_2B_3H_2$-5-Me)$^{2-}$ and 2,3-$Et_2C_2B_4H_4{}^{2-}$ dianions with $CoCl_2$ gave the diamagnetic 30 ve (valence electron) triple-decker Cp*Co($Et_2C_2B_3H_2$Me)CoH($Et_2C_2B_4H_4$) (**2**) and the paramagnetic 29 ve triple-decker Cp*Co($Et_2C_2B_3H_2$Me)Co($Et_2C_2B_4H_4$) (**3**). Decapitation of these species gave diamagnetic Cp*Co($Et_2C_2B_3H_2$Me)CoH($Et_2C_2B_3H_5$) (**4**), whose triple-decker geometry was confirmed by an X-ray structure determination that established the location of the hydrogen atom capping a CoB_2 triangular face. Removal of the CoH proton in **4** followed by oxidation of the anion in air gave paramagnetic Cp*Co($Et_2B_3H_2$Me)Co($Et_2C_2B_3H_5$) (**5**). Treatment of neutral **4** and **5** with *n*-bromosuccinimide afforded the mono- and dibromo derivatives **6–8**. The 30 ve triple-decker Cp*Co($Et_2C_2B_3Me_3$)Ni($Et_2C_2B_4H_4$) (**10**) was prepared from the peralkylated synthon Cp*Co(2,3-$Et_2C_2B_3Me_3$)$^{2-}$, $Et_2C_2B_4H_4{}^{2-}$, and $NiBr_2$. A similar approach employing the cymeneruthenacarborane dianion ($CHMe_2C_6H_4$Me)Ru($Et_2C_2B_3H_2$Me)$^{2-}$ gave the paramagnetic triple-decker ($CHMe_2C_6H_4$Me)Ru($Et_2C_2B_3H_2$Me)Co($Et_2C_2B_4H_4$) (**12**), which was decapitated to yield diamagnetic ($CHMe_2C_6H_4$Me)Ru($Et_2C_2B_3H_2$Me)CoH($Et_2C_2B_3H_5$) (**13**); the latter species was air-oxidized to afford 29 ve ($CHMe_2C_6H_4$Me)Ru($Et_2C_2B_3H_2$Me)Co($Et_2C_2B_3H_5$) (**14**). Stacking reactions of the nido, closo dianion ($Et_2C_2B_3H_4$Me)Co($Et_2C_2B_4H_4$)$^{2-}$ (**15**$^{2-}$) with Co^{2+} or Ni^{2+} ions gave the paramagnetic carborane-bicapped tetradecker sandwiches M[($Et_2C_2B_3H_2$Me)Co($Et_2C_2B_4H_4$)]$_2$ (**16**, M = Co, 41 ve; **17**, M = NiH, 43 ve). Reactions of the **15**$^{3-}$ trianion with Cp*Co(2,3-$Et_2C_2B_3H_2$Me)$^{2-}$ ion and Co^{2+} or Ni^{2+} gave the carborane-monocapped tetradeckers Cp*Co($Et_2C_2B_3H_2$Me)M($Et_2C_2B_3H_2$Me)CoH($Et_2C_2B_4H_4$) (**18**, M = Co, 41 ve; **19**, M = Ni, 42 ve, diamagnetic). Decapitation of **18** gave paramagnetic 41 ve Cp*Co($Et_2C_2B_3H_2$Me)Co($Et_2C_2B_3H_2$Me)CoH($Et_2C_2B_3H_5$) (**20**), a 41 ve tetradecker sandwich having an open carborane end ligand. The new compounds were characterized via UV–visible and mass spectra, ^1H and ^{11}B NMR spectra (for diamagnetic species), and ESR spectra (for paramagnetic complexes). Features of the spectroscopic data are discussed and related to the electronic structures of these systems. Crystal data for **4**: space group $P2_1/a$; $a = 9.312(3)$ Å, $b = 28.25(1)$ Å, $c = 10.234(4)$ Å, $\beta = 95.56(3)°$; $Z = 4$; $R = 0.048$ for 3834 independent reflections having $I > 3\sigma(I)$.

Introduction

Multidecker metal sandwich complexes that are stabilized by bridging heterocycles such as carborane (C_2B_3),[3] organoboron (C_3B_2, C_2B_2S, C_4B, C_4B_2),[4] or E_n (E = P, As)[5] rings form a large, diverse, and rapidly expanding area of organometallic chemistry that is of potential interest in the development of new electroactive materials. In the metallacarborane area, triple-decker and tetradecker sandwiches incorporating C_2B_3 ligands (formally $RR'C_2B_3H_3{}^{4-}$ or B-substituted derivatives thereof) are prepared from suitably derivatized double-decker *nido*-LM($RR'C_2B_3H_5$) complexes, as shown in Scheme 1.[1a,3] The versatility of these stacking reactions has allowed us to prepare a variety of multideckers incorporating first-, second-, and third-row transition metals, and the complexes obtained are in most cases air-stable crystalline solids whose metal centers can undergo reversible changes in oxidation state. Moreover, the double-decker building-block compounds are readily functionalized via introduction of halogens or organic groups on the carborane ring, thereby enabling the synthesis of specifically tailored multidecker sandwiches.[6] However, there is an inherent limitation in this approach: the end-capping hydrocarbon ring ligands (Cp, Cp* [η^5-C_5Me_5], or arene) in these compounds are apparently inert toward further sandwich complexation with metal ions. Thus, although linked-sandwich oligomers connected via covalent single bonds between end ligands have been prepared[1b,7] (e.g., Chart 1, A and B), multidecker stacking of hydrocarbon-capped metallacarboranes with metal ions (e.g.,

---

[⊗] Abstract published in *Advance ACS Abstracts,* December 1, 1995.

(1) (a) Part 42: Wang, X.; Sabat, M.; Grimes, R. N. *Inorg. Chem.* In press. (b) Part 41: Wang, X.; Sabat, M.; Grimes, R. N. *Organometallics* **1995,** *14,* 4668. (c) Part 40: Stockman, K. E.; Garrett, D. L.; Grimes, R. N. *Organometallics* **1995,** **14,** 4661.

(2) Based in part on the Ph.D. dissertation of X.W., University of Virginia, 1995.

(3) (a) Grimes, R. N. *Chem. Rev.* **1992,** *92,* 251. (b) Grimes, R. N. In *Current Topics in the Chemistry of Boron*; Kabalka, G. W., Ed.; Royal Society of Chemistry; 1994; p 269. Closely related C_2B_4-metal chemistry has also recently been reviewed: (c) Hosmane, N. S.; Maguire, J. A. *J. Cluster Sci.* **1993,** *4,* 297. (d) Saxena, A. K.; Hosmane, N. S. *Chem. Rev.* **1993,** **93,** 1081.

(4) (a) Siebert, W. *Adv. Organomet. Chem.* **1993,** *35,* 187. (b) Siebert, W. *Angew. Chem., Int. Ed. Engl.* **1985,** *24,* 943. (c) Herberich, G. E.; Carstensen, T.; Koeffer, D. P. J.; Klaff, N.; Boese, R.; Hyla-Krypsin, I.; Gleiter, R.; Stephan, M.; Meth, H.; Zenneck, U. *Organometallics* **1994,** *13,* 619 and references therein. (d) Herberich, G. E In *Comprehensive Organometallic Chemistry*: Wilkinson, G., Stone, F. G. A., Abel, E., Eds.; Pergamon Press: Oxford, 1995; Vol. II, Chapter 1.5. (e) Kuhlmann, T.; Pritzkow, H.; Zenneck, U.; Siebert, W. *Angew. Chem., Int. Ed. Engl.* **1984,** *23,* 965. (f) Zwecker, J.; Kuhlmann, T.; Pritzkow, H.; Siebert, W.; Zenneck, U. *Organometallics* **1988,** *7,* 2316. (g) Fessenbecker, A.; Hergel, A.; Hettrich, R.; Schaefer, V.; Siebert, W. *Chem. Ber.* **1993,** *126,* 2205. (h) Weinmann, W.; Wolf, A.; Pritzkow, H.; Siebert, W.; Barnum, B. A.; Carroll, P. J.; Sneddon, L. G. *Inorg. Chem.* **1995,** *14,* 1911.

(5) Scherer, O. J. *Angew. Chem. Internat. Edit. Engl.* **1990,** *29,* 1104.

(6) (a) Davis, J. H., Jr.; Attwood, M. D.; Grimes, R. N. *Organometallics* **1990,** *9,* 1171. (b) Piepgrass, K. W.; Grimes, R. N. *Organometallics* **1992,** *11,* 2397. (c) Piepgrass, K. W.; Stockman, K. E.; Sabat, M.; Grimes, R. N. *Organometallics* **1992,** *11,* 2404. (d) Benvenuto, M. A.; Grimes, R. N. *Inorg. Chem.* **1992,** *31,* 3897. (e) Benvenuto, M. A.; Sabat, M.; Grimes, R. N. *Inorg. Chem.* **1992,** *31,* 3904.

0002-7863/95/1517-12218\$09.00/0

Scheme 1

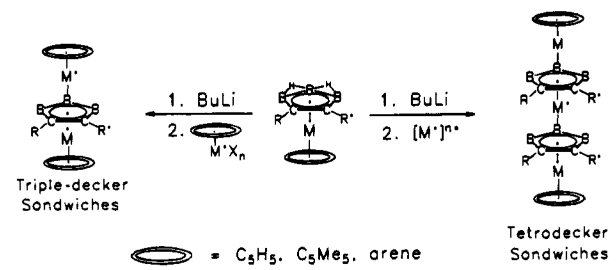

M = Fe, Co, Ru, Rh, Ir

M' = Co, CoH, Ni, Ru, Rh, Os, Ir

B = BH, B-alkyl, B-Cl, B-Br, B-I

R, R' = alkyl, SiMe$_3$

Chart 1

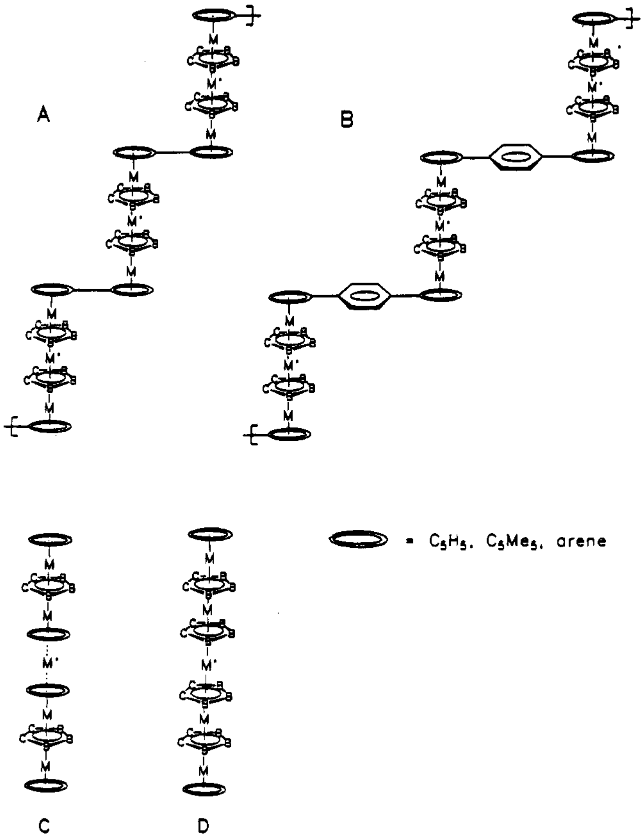

C) has not been observed and appears unlikely as a viable synthetic strategy. Consequently, in order to construct metallacarborane sandwiches of more than four decks, one clearly wants triple-decker (or larger) synthons having open C_2B_3 end rings that are amenable to further stacking (Chart 1, D). In this paper we report the synthesis and characterization of a number of species of this type, with their subsequent use in the preparation of penta- and hexadecker sandwiches described in the accompanying report.[8]

Results and Discussion

Synthesis of Carborane-End-Capped Triple-Decker Sandwiches. Complexes of the target type containing $M(C_2B_3)$ end units cannot be prepared directly from planar C_2B_3 ring ligands, since uncomplexed carboranes of the latter class are not available in solution; hence they are generated from $M(C_2B_4)$ complexes via removal of the apex BH unit (decapitation), a well-established method.[3a,b] In the present study, the C_2B_4-capped triple-deckers **2** and **3** were synthesized in a combined 60% yield by reaction of the $Cp^*Co(2,3\text{-}Et_2C_2B_3H_2\text{-}5\text{-}Me)^{2-}$ ($\mathbf{1a}^{2-}$) and $2,3\text{-}Et_2C_2B_4H_4^{2-}$ dianions with cobaltous ion followed by workup in air on silica columns, as depicted in Scheme 2. (In this and subsequent schemes, formal oxidation states are assigned as an aid in discussions of the chemistry and NMR data). The corresponding reaction involving the *mono*anions $Cp^*Co(Et_2C_2B_3H_4)^-$ and $Et_2C_2B_4H_5^-$ affords the same products,[9] but is sensitive to reaction conditions and gives varying yields. The presence of a B-methyl group in the double-decker complex is important in blocking oxidative fusion[10] of the ligands; analogous reactions of unsubstituted CoC_2B_3 and CoC_2B_4 anions afford fused clusters.[11]

Scheme 2

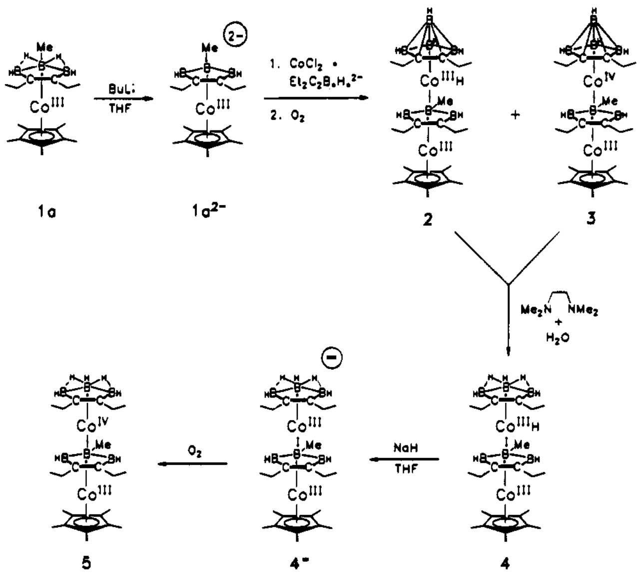

Compounds **2** and **3** were characterized from NMR or ESR data, UV–visible and mass spectra, and elemental analysis as C_2B_4-capped triple-decker sandwiches, structurally similar to the C_3B_3-capped triple-deckers and tetradeckers reported earlier by Siebert and co-workers.[4e–g] (Triple-deckers having large C_3B_7 carborane end units have also been described recently.[4h]) Tables 1–3 list ^{1}H and ^{11}B NMR shifts for the diamagnetic products and UV–visible absorptions for all new compounds. Complex **2** is a brown diamagnetic solid having 30 valence electrons (ve),[12] corresponding to the assignment of +3 formal oxidation states for both cobalt atoms and formal −2, −4, and −1 charges for the C_2B_4, C_2B_3, and Cp* ligands, respectively. Electroneutrality of this species is afforded by the proton associated with one of the cobalt centers, whose ^{1}H NMR signal at ca. δ −9 is clearly evident. In the proton-coupled ^{11}B NMR spectrum, the singlet peak at δ 14 is assigned to the methylated boron B(5).

Compound **3**, a 29 ve paramagnetic system, has one less hydrogen than **2** and contains formal Co(III) and Co(IV) centers. Its X-band ESR spectrum at 115 K is well-resolved and exhibits

---

(7) (a) Meng, X.; Sabat, M.; Grimes, R. N. *J. Am. Chem. Soc.* **1993**, *115*, 6143. (b) Davis, J. H., Jr.; Benvenuto, M.; Grimes, R. N. *Inorg. Chem.* **1991**, *30*, 1765.

(8) Wang, X.; Sabat, M.; Grimes, R. N. *J. Am. Chem. Soc.* **1995**, *117*, 12227–12234.

(9) Waterworth, S.; Grimes, R. N. Third Boron U.S.A. Workshop, Washington State University, Pullman, WA, July 1992; Abstract 51.

(10) (a) Piepgrass, K. W.; Curtis, M. A.; Wang, X.; Meng, X.; Sabat, M.; Grimes, R. N. *Inorg. Chem.* **1993**, *32*, 2156. (b) Grimes, R. N. *Coord. Chem. Rev.* **1995**, *143*, 71 and references therein.

(11) Wang, X.; Grimes, R. N. Unpublished observations.

(12) The formal $Et_2C_2B_3H_3^{4-}$ and $Et_2C_2B_4H_4^{2-}$ ligands are both 6-electron donors analogous to $C_5Me_5^-$.

Table 1. 115.8-MHz ^{11}B FT NMR Data

compound	δ (J_{BH}, Hz)$^{a-c}$
$Cp^*Co(Et_2C_2B_3H_2Me)CoH(Et_2C_2B_4H_4)$ (**2**)	14.0, 5.6 (137), 1.6 (139), −2.5, −3.9
$Cp^*Co(Et_2C_2B_3H_2Me)CoH(Et_2C_2B_3H_5)$ (**4**)	22.5, 1.6 (96), −1.9
$Cp^*Co(Et_2C_2B_3H_2Me)CoH(Et_2C_2B_3H_4$-4-Br) (**6**)	22.3, 9.2, 1.5
$Cp^*Co(Et_2C_2B_3Me_3)Ni(Et_2C_2B_4H_4)$ (**10**)	20.2 (138), 16.6, 4.1 (139), 1.4
$(CHMe_2C_6H_4Me)Ru(Et_2C_2B_3H_2Me)CoH(Et_2C_2B_3H_5)$ (**13**)	14.6, 1.7 (109), −4.4
$(Et_2C_2B_3H_4Me)CoH(Et_2C_2B_4H_4)$ (**15**)	14.1, −2.3 (138), −6.3 (161), −7.8, −16.3
$Cp^*Co(Et_2C_2B_3H_2Me)Ni(Et_2C_2B_3H_2Me)CoH(Et_2C_2B_4H_4)$ (**19**)	51.7, 43.2, 19.6, 2.6, −1.3, −3.5, −10.7

[a] Shifts relative to $BF_3\cdot OEt_2$, positive values downfield. [b] Dichloromethane solution. [c] H−B coupling constant in Hz is given in parentheses, when resolved. Peak broadness and overlap prevent accurate determination of relative areas.

Table 2. 300-MHz ^{1}H FT NMR Data

compd	δ^{a-c}
2	2.53 m (CH_2), 2.32 m (CH_2), 2.17 m (CH_2), 1.60 t (ethyl CH_3), 1.52 s (C_5Me_5), 1.12 t (ethyl CH_3), 0.75 s (B−CH_3), −9.0 s (CoH)
4	2.37 m (CH_2), 1.96 m (CH_2), 1.60 s (C_5Me_5), 1.45 t (ethyl CH_3), 0.98 t (ethyl CH_3), 0.79 s (B−CH_3), −6.4 s, br (BHB, CoH)
6	2.35 m (CH_2), 2.10 m (CH_2), 1.60 s (C_5Me_5), 1.46 t (ethyl CH_3), 0.91 m (ethyl CH_3), 0.77 s (B−CH_3), −4.5 s, br (BHB), −5.9 s, br (BHB), −6.1 s, br (CoH)
10	2.74 m (CH_2), 2.58 m (CH_2), 2.40 m (CH_2), 2.22 m (CH_2), 1.46 s (B−CH_3), 1.41 t (ethyl CH_3), 1.52 s (C_5Me_5), 0.91 t (ethyl CH_3), 0.67 s (B−CH_3)
13	4.94 m (C_6H_4), 2.60 m (CH_2), 2.21 m (CH_2), 2.09 s (cymene CH_3), 2.02 m (cymene CH), 1.34 t (ethyl CH_3), 1.23 d (cymene CH_3), 1.01 t (ethyl CH_3), 0.66 s (B−CH_3), −5.6 s, br (CoH), −6.3 s, br (BHB)
15	2.54 m (CH_2), 2.28 m (CH_2), 2.17 m (CH_2), 1.99 m (CH_2), 1.18 t (ethyl CH_3), 1.07 t (ethyl CH_3), 0.59 s (B−CH_3), −4.9 s, br (BHB), −6.2 s, br (CoH)
19	1.88−2.62 m (CH_2), 1.66 s (C_5Me_5), 1.53 d (B−CH_3), 1.42 s (B−CH_3), 1.14 t (ethyl CH_3), 1.02 t (ethyl CH_3), 0.82 t (ethyl CH_3), −4.6 s, br (CoH)

[a] $CDCl_3$ solution. [b] Shifts relative to $(CH_3)_4Si$. Integrated peak areas in all cases are consistent with the assignments given. Legend: m = multiplet, s = singlet, d = doublet, t = triplet, q = quartet. [c] B−$H_{terminal}$ resonances are broad quartets and mostly obscured by other signals.

Table 3. UV−Visible Absorptions (CH_2Cl_2 Solution)

compd	λ, nm (rel intensity in parentheses)
2	238 (61), 342 (100)
3	234 (51), 270 (47), 340 (100)
4	280 (30), 336 (100), 454 (11)
5	336 (100), 546 (9)
6	234 (65), 352 (100)
7	278 (31), 352 (100)
8	234 (74), 328 (77), 366 (100)
10	232 (39), 252 (40), 302 (52), 372 (100)
12	232 (37), 284 (100)
13	286 (78), 310 (100)
14	234 (95), 248 (100), 308 (84)
15	234 (87), 282 (100)
16	292 (80), 346 (90), 364 (100), 514 (20)
17	234 (100), 286 (100), 354 (42), 430 (34)
18	292 (83), 376 (100)
19	292 (80), 372 (100), 554 (35), 664 (20)
20	298 (71), 378 (100)

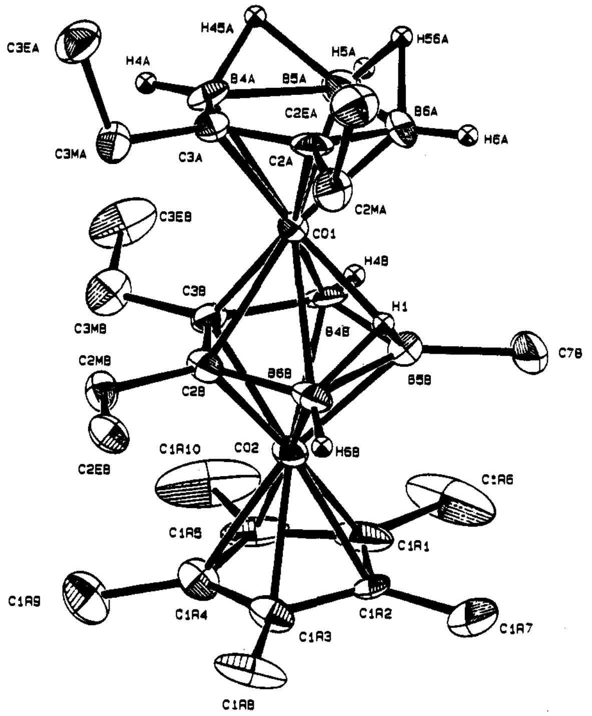

Figure 1. Molecular structure of **4**.

an isotropic **g** tensor of 2.13, consistent with the presence of one unpaired electron associated with a d^5 [Co(IV)] metal. No Co hyperfine structure is seen, suggesting that the unpaired electron density may be partially delocalized between the two metals. If the MO calculations by Lauher et al.[13] on triple-decker systems, subsequently modified by Merkert and coworkers for RuRu and CoRu complexes,[14] are used as a model in the present case, the HOMOs can be assigned as a degenerate pair having e_2'' symmetry and derived from the d_{xy} and $d_{x^2-y^2}$ metal orbitals. The electronic spectrum of **3** contains an extra band at 270 nm that does not appear in that of **2**, and is assumed to arise from excitation of an electron in a lower-energy MO to the single vacancy in the degenerate HOMOs of **3** (further discussion of UV−visible data in these and other compounds is presented below).

Decapitation of **2** and **3** with wet tetra-*N*-methylethylenediamine (TMEDA) gave $Cp^*Co(Et_2C_2B_3H_2Me)CoH(Et_2C_2B_3H_5)$ (**4**, Scheme 2). Characterization of this 30 ve diamagnetic compound by NMR spectroscopy was straightforward, and its triple-decker geometry was confirmed by X-ray crystallography. The structure of **4** is presented in Figure 1, with data collection parameters listed in Table 4 and bond distances and angles in Table 5. This structure determination is the first available for a multidecker complex having a C_2B_3 end ring, and fortunately the data permitted refinement of all hydrogen atoms including that associated with cobalt [H(1)]. Viewed as a cluster system, this molecule consists of a closo 7-vertex CoC_2B_3Co polyhedron and a nido 6-vertex CoC_2B_3 unit sharing a common cobalt atom, with both cage geometries exhibiting normal features for small

---

[13] Lauher, J. W.; Elian, M.; Summerville, R. H.; Hoffmann, R. *J. Am. Chem. Soc.* **1976**, *98*, 3219.

[14] Merkert, J.; Davis, J. H., Jr.; Geiger, W.; Grimes, R. N. *J. Am. Chem.Soc.* **1992**, *114*, 9846.

Table 4. Experimental X-ray Diffraction Parameters and Crystal Data for **4**

empirical formula	$Co_2C_{23}B_6H_{46}$
formula wt	503.3
crystal color, habit	dark prism
crystal dimensions (mm)	0.32 × 0.34 × 0.48
space group	$P2_1/a$
a, Å	9.312(3)
b, Å	28.25(1)
c, Å	10.234(4)
β, deg	95.56(3)
V, Å^3	2680
Z	4
μ, cm^{-1} (Mo Kα)	12.45
transmission factors	0.89–1.00
D(calcd), g cm^{-3}	1.253
$2\theta_{max}$, deg	46.0
reflctns measd	4095
reflctns obsd [$I > 3\sigma(I)$]	3834
R	0.048
R_w	0.076
largest peak in final diff map, e/Å^3	0.46

Scheme 3

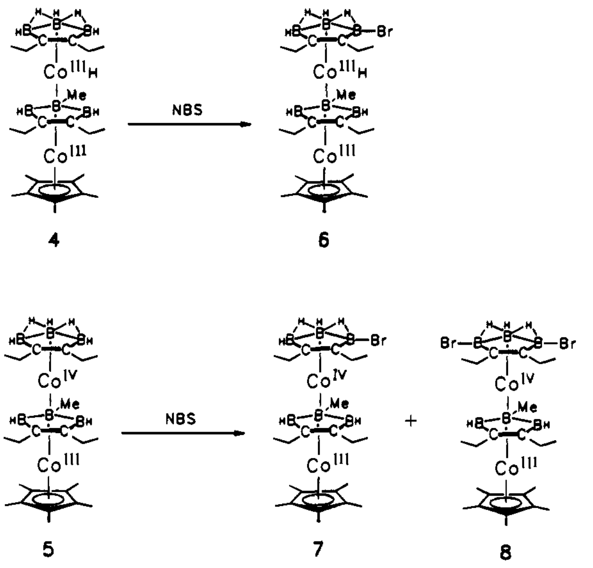

metallacarboranes (except for the effects of the face-bridging hydrogen H(1), noted below). For example, the short C–C distance in the open ring [C(2A)–C(3A), 1.413(9) Å] compared to that in the closo cluster [C(2B)–C(3B), 1.467(9) Å] is typical, and reflects the higher coordination of the latter carbons.

The triple-decker sandwich geometry is significantly distorted with a dihedral angle of 12° between the two C_2B_3 rings, such that the outer (end) ligand is bent away from the Co–B(5B)–B(6B) face that accommodates the bridging hydrogen H(1). The bending is attributed to a tilting of the Co(1) d_{z^2} orbital (or a hybrid thereof) in order to achieve optimal overlap of its lower lobe with H(1). The Cp* and middle C_2B_3 rings are nearly parallel with a dihedral angle of 4.9°. The unique hydrogen H(1) is much closer to its boron neighbors [B(5B)–H(1), 1.35(7) Å; B(6B)–H(1), 1.32(7) Å] than it is to Co(1) [1.77(7) Å]; indeed, these B–H–B distances are closely comparable to those found for the B–H–B hydrogens on the open face [H(45A) and H(56A)]. The lone precedent for a crystallographically defined face-capping hydrogen in *metallacarborane* chemistry[15] is found in the dinuclear ferracarborane[16] $[(Et_2C_2B_4H_4)FeH(C_5Me_4)]_2C_6H_4$. In that species, each bridging hydrogen is 1.63 Å from iron and ca. 1.45 Å from the nearest boron atoms, somewhat closer to a true face-bridging situation than is the case in **4**. Possibly, the lower formal oxidation state [Fe(II)] in the iron species favors covalent metal–hydrogen binding in the latter case more than does Co(III) in **4**. Another feature noted in the ferracarborane[16]—longer than normal metal–boron and boron–boron distances in the M–B–B triangle containing the face-bridging proton—is also apparent in **4**: thus, B(5B)–B(6B) and Co(1)–B(6B) are each ca. 0.2 Å greater than their non-H-bridged counterparts B(5B)–B(4B) and Co(1)–B(4B). In both structures, it is evident that some electron density in the affected triangles is diverted to the face-bonded hydrogen, weakening the M–B and B–B interactions.

The location of H(1) in solutions of **4** is less clear, although tautomeric interchange between the two equivalent B–Co–B faces is likely. The proton NMR signal of H(1) is unfortunately superimposed on that of the B–H–B hydrogens on the open face, giving a broad peak at δ −6.4. In the ^{11}B NMR spectrum, overlap of two resonances leads to a simpler than expected pattern having three rather than four peaks.

Both types of bridge hydrogens in **4** exhibit acidic character in solution, that of H(1) being stronger; thus, deprotonation of **4** with alkyllithium reagents or metal hydrides removes H(1) but not the BHB protons on the open face (Scheme 2). The presence of these bridging hydrogens in the **4**$^-$ anion effectively blocks metal complexation of that anion, and thereby precludes its use *per se* as a synthon for constructing larger stacks. However, the problem was circumvented by air-oxidation of **4**$^-$ to neutral **5** as illustrated in Scheme 2.[17] Complex **5**, a dark brown paramagnetic solid, lacks a metal-bound (face-bridging) proton and consequently the open-face BHB protons can be removed by standard methods, opening the way to metal complexation and stacking.[8] The ESR spectrum of **5**, a formal 29-electron triple-decker, is similar to that of **3** obtained under identical conditions (isotropic **g** tensor = 2.11, no Co hyperfine splitting), supporting the electronic analogy between these species.

The open faces in both **4** and **5** can be derivatized via methods previously employed for the corresponding double-decker sandwich complexes such as $Cp^*Co(Et_2C_2B_3H_5)$.[6] Thus, treatment of each species with *N*-bromosuccinimide (NBS) readily generated the dark brown brominated products **6**–**8** (Scheme 3). Interestingly, in the case of **6** the face-bound proton remains intact and its ^1H chemical shift is essentially unchanged compared to **4**. However, the asymmetry introduced by the bromine substituent in **6** is evident in the observation of two distinct open-face BHB proton NMR resonances.

Preparation of Nickel and Ruthenium Triple-Decker Sandwiches. The approach employed in the synthesis of the dicobalt triple-deckers was extended to other metals. Since Ni is isoelectronic with the CoH moiety, an attempt was made to prepare the diamagnetic Ni(IV)–Co(III) analogue of **2**, $Cp^*Co(Et_2C_2B_3H_2\text{-}Me)Ni(Et_2C_2B_4H_4)$, via reaction of **1a**$^{2-}$ with the $Et_2C_2B_4H_4^{2-}$ dianion and $NiBr_2$. However, the only product detected via mass spectrometry lacked nickel and corresponded to the formula $Cp^*Co(Et_2C_2B_7H_7)$ (**9**), suggesting that the target NiCo complex may have formed and undergone oxidative fusion on workup; this product was not further characterized. More successful was the preparation of the nickel–cobalt triple-decker

---

(15) In metallaboranes (exclusive of carboranes), the locations of hydrogen atoms capping Co_2B or CoB_2 faces have been established in a few instances. See: (a) Pipal, J. R.; Grimes, R. N. *Inorg. Chem.* **1977**, *16*, 3255. (b) Pipal, J. R.; Grimes, R. N. *Inorg. Chem.* **1979**, *18*, 252. (c) Feilong, J.; Fehlner, T. P.; Rheingold, A. L. *J. Am. Chem. Soc.* **1987**, *109*, 1860.

(16) Stephan, M.; Davis, J. H., Jr.; Meng, X.; Chase, K. P.; Hauss, J.; Zenneck, U.; Pritzkow, H.; Siebert, W.; Grimes, R. N. *J. Am. Chem. Soc.* **1992**, *114*, 5214.

(17) A preliminary account of part of this work has appeared: Wang, X.; Sabat, M.; Grimes, R. N. *J. Am. Chem. Soc.* **1994**, *116*, 2687.

Table 5. Bond Distances and Selected Bond Angles for $Cp^*Co(Et_2C_2B_3H_2Me)CoH(Et_2C_2B_3H_5)$ (**4**)

Bond Distances, Å

Co(1)–C(2A)	2.110(6)	C(2MA)–C(2A)	1.51(1)	C(1R1)–C(1R2)	1.38(1)
Co(1)–C(2B)	2.105(6)	C(2MA)–C(2EA)	1.53(1)	C(1R1)–C(1R5)	1.42(1)
Co(1)–C(3A)	2.123(6)	C(2A)–C(3A)	1.413(9)	C(1R1)–C(1R6)	1.53(1)
Co(1)–C(3B)	2.093(6)	C(2A)–B(6A)	1.54(1)	C(1R2)–C(1R3)	1.41(1)
Co(1)–B(4A)	2.051(8)	C(2B)–C(2MB)	1.514(9)	C(1R2)–C(1R7)	1.52(1)
Co(1)–B(4B)	2.076(8)	B(5A)–B(6A)	1.82(1)	C(1R3)–C(1R4)	1.41(1)
Co(1)–B(5A)	2.028(8)	B(5A)–H(5A)	1.08(6)	C(1R3)–C(1R8)	1.50(1)
Co(1)–B(5B)	2.259(8)	B(5A)–H(56A)	1.33(5)	C(1R4)–C(1R5)	1.42(1)
Co(1)–B(6A)	2.034(8)	B(5B)–B(6B)	1.84(1)	C(1R4)–C(1R9)	1.47(1)
Co(1)–B(6B)	2.274(8)	B(5B)–H(1)	1.35(7)	C(1R5)–C(1R10)	1.52(1)
Co(1)–H(1)	1.77(7)	C(2B)–C(3B)	1.467(9)	B(4A)–B(5A)	1.81(1)
Co(2)–C(2B)	2.058(6)	C(2B)–B(6B)	1.55(1)	B(4A)–H(4A)	1.05(9)
Co(2)–C(3B)	2.051(6)	C(2MB)–C(2EB)	1.52(1)	B(4A)–H(45A)	1.30(10)
Co(2)–C(1R1)	2.030(8)	C(3A)–C(3MA)	1.513(9)	B(4B)–B(5B)	1.66(1)
Co(2)–C(1R2)	2.028(7)	C(3A)–B(4A)	1.52(1)	B(4B)–H(4B)	1.07(8)
Co(2)–C(1R3)	2.071(7)	C(3MA)–C(3EA)	1.53(1)	B(5A)–H(45A)	1.50(10)
Co(2)–C(1R4)	2.086(6)	C(3MB)–C(3B)	1.53(1)	B(6A)–H(56A)	1.38(6)
Co(2)–C(1R5)	2.064(7)	C(3MB)–C(3EB)	1.55(1)	B(6A)–H(6A)	0.90(6)
Co(2)–B(4B)	2.097(7)	C(3B)–B(4B)	1.57(1)	B(6B)–H(1)	1.32(7)
Co(2)–B(5B)	2.083(8)	C(7B)–B(5B)	1.61(1)	B(6B)–H(6B)	1.12(5)
Co(2)–B(6B)	2.049(8)				

Selected Bond Angles, deg

Co(1)–C(2A)–C(2MA)	126.8(5)	C(2B)–C(3B)–C(3MB)	120.0(6)
C(2MA)–C(2A)–C(3A)	124.7(6)	C(2B)–C(3B)–B(4B)	110.7(6)
C(2MA)–C(2A)–B(6A)	120.1(7)	C(3MB)–C(3B)–B(4B)	129.3(6)
C(3A)–C(2A)–B(6A)	114.7(6)	C(3B)–C(3MB)–C(3EB)	114.2(6)
C(2A)–C(2MA)–C(2EA)	111.6(6)	C(3A)–B(4A)–B(5A)	106.5(7)
Co(1)–C(3A)–C(3MA)	130.9(4)	B(4A)–B(5A)–B(6A)	96.9(6)
C(2A)–C(3A)–C(3MA)	122.9(6)	C(2A)–B(6A)–B(5A)	106.1(6)
C(2A)–C(3A)–B(4A)	115.7(6)	C(3B)–B(4B)–B(5B)	109.9(6)
C(3MA)–C(3A)–B(4A)	121.2(6)	B(4B)–B(5B)–B(6B)	100.4(6)
C(3A)–C(3MA)–C(3EA)	111.0(6)	Co(1)–B(5B)–C(7B)	130.9(6)
Co(1)–C(2B)–C(2MB)	129.8(4)	Co(2)–B(5B)–C(7B)	133.4(6)
Co(2)–C(2B)–C(2MB)	128.7(4)	C(7B)–B(5B)–B(4B)	131.7(7)
C(2MB)–C(2B)–C(3B)	119.9(6)	C(7B)–B(5B)–B(6B)	127.8(7)
C(2MB)–C(2B)–B(6B)	124.6(6)	C(2B)–B(6B)–B(5B)	103.3(6)
C(3B)–C(2B)–B(6B)	115.3(5)	B(6B)–H(1)–B(5B)	87(4)
C(2B)–C(2MB)–C(2EB)	114.3(6)	B(4A)–H(45A)–B(5A)	81(6)
Co(1)–C(3B)–C(3MB)	129.0(5)	B(5A)–H(56A)–B(6A)	84(3)
Co(2)–C(3B)–C(3MB)	128.9(5)		

10 from the trimethylated dianion **1b**$^{2-}$ as shown in Scheme 4. This product was isolated as a diamagnetic red-brown solid and characterized from NMR, UV–visible, and mass spectroscopic data. Interpretation of its proton NMR spectrum (Table 2) is straightforward and reveals that the methyl resonances have all shifted downfield from their values in the neutral precursor *nido*-$Cp^*(Et_2C_2B_3Me_3)$ (**1b**);[6a] those of the "outer" methyl groups [attached to B(4) and B(6)] are deshielded by ca. 0.50 ppm in **10** relative to **1b**, while the central B(4)-methyl signal moves downfield by nearly 1.1 ppm, implying that the middle boron in **1b** is more strongly affected (deshielded) by metal complexation than are the side borons.

An attempted decapitation of **10** by treatment with TMEDA in the usual way led to decomposition of most of the starting material, and an alternative approach using acidified acetate gave only a fused product.

The general strategy employed for the cobalt-containing species was applied in this study to the arene–ruthenium sandwich[6a] *nido*-(cymene)$Ru(Et_2C_2B_3H_5)$ (cymene = *p*-isopropyltoluene), an isoelectronic analogue of *nido*-$Cp^*Co(Et_2C_2B_3H_5)$ that has been employed in earlier work to prepare arene-capped triple-deckers.[18,19] Reaction of the monomethylated dianion **11**$^{2-}$ with the carborane dianion afforded on workup the paramagnetic product **12** (Scheme 4), which is formulated as a Ru(II)–Co(IV) system by analogy with related CoRu triple-deckers in which the unpaired electron resides mainly on cobalt.[14] Although **12** is an isoelectronic counterpart of the dicobalt species **3**, the corresponding diamagnetic Ru(II)–Co(III)H species analogous to **2** was not detected.

The X-band ESR spectrum of **12** at 115 K in CH_2Cl_2 gives $g_\parallel$ and $g_\perp$ values of 3.28 and 2.13, respectively, with no resolved cobalt hyperfine structure. Notably, the axial symmetry of the **g** tensor of this complex differs from the spherical symmetry of the **g** tensors of the dicobalt triple-deckers **3** and **5** (vide supra) despite the fact that the three species are isoelectronic. We interpret this difference as a consequence of lower ligand field symmetry in the heterobimetallic RuCo system.

Decapitation of **12** with TMEDA proceeded smoothly to generate the red-brown diamagnetic Co(III)H–Ru(II) complex **13**, as shown. Complex **13** is an analogue of the dicobalt triple-decker **4**, and their ^1H and ^{11}B NMR spectra are somewhat similar (Tables 1 and 2); however, the shift of the CoH proton in **13**, in contrast to that of **4**, is clearly distinct from the BHB signal, appearing well downfield from the latter at δ −5.6. The ^{11}B NMR spectrum of **13** is better resolved than that of **4**, with the resonance of the methylated boron [B(5)] appearing at δ 14.6. Deprotonation and subsequent oxidation of **13**, as in the case of **4**, gave the paramagnetic neutral complex **14**, obtained as a dark green solid. The X-band ESR spectrum of this compound exhibits axial symmetry with $g_\parallel$ and $g_\perp$ values of 2.21 and 2.03, respectively, with partial overlap between these

---

(18) Davis, J. H., Jr.; Sinn, E.; Grimes, R. N. *J. Am. Chem. Soc.* **1989**, *111*, 4776.

(19) Greiwe, P.; Sabat, M.; Grimes, R. N. *Organometallics* **1995**, *14*, 3683.

Scheme 4

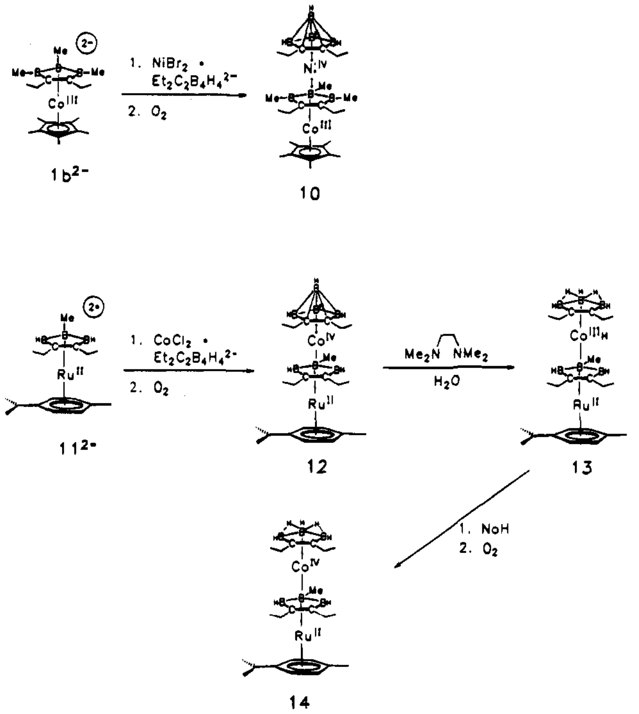

signals. In this case, hyperfine structure is seen in the parallel signal, indicating some association of the unpaired electron density with cobalt. These findings can be compared with those for the 29 ve cation $CpCo(Et_2C_2B_3H_3)Ru(cymene)^+$, whose ESR spectrum also exhibits hyperfine structure (although to a lesser degree than the 31 ve monoanion of that complex).[14]

Synthesis of Carborane-End-Capped Tetradecker Sandwiches. *nido,closo*-$(R_2C_2B_3H_5)M(R'_2C_2B_4H_4)$ metallacarborane sandwich complexes[20,21] such as **15** (Scheme 5) are particularly useful synthons for sandwich building in that they are nearly isostructural with metallocenes, as illustrated by their incorporation in the first metallocenium–metallacarboraneide "mixed-sandwich" salts.[21] Earlier attempts in our laboratory to prepare tetradecker complexes from unsubstituted substrates of the nido-closo type had led only to fused products.[9] However, since it has been found[22] that metal stacking with $Cp^*Co(Et_2C_2B_3H_4\text{-}5\text{-}X)$ complexes is strongly affected by the choice of X substituent, and works particularly well when X is acetyl, halogen, or methyl, we employed the B(5)-methylated species **15**[21] to construct tetradecker complexes as outlined in Scheme 5.

Complex **15** contains three acidic hydrogens, and hence one can generate the mono- di-, or trianion as desired via addition of 1–3 equiv of base. The dianion $\mathbf{15}^{2-}$ reacted with cobaltous or nickelous ion to form, on workup in air, the corresponding carborane-bicapped tetradecker sandwiches $M[(Et_2C_2B_3H_2Me)Co(Et_2C_2B_4H_4)]_2$ (**16**, M = Co; **17**, M = NiH) in isolated yields of 70% and 35%, respectively. Both products were obtained as somewhat air-sensitive black oily solids and were characterized from their mass spectra, UV–visible spectra, and elemental analysis. The mass spectra exhibit very strong parent ion envelopes whose intensity patterns correspond to the structures proposed in Scheme 5, with two metal-bound hydrogens in **16** and three in **17**. Formulated in this way, **16** and **17** are 41 and 43 ve systems, respectively, in agreement with the paramagnetism implied by their NMR spectra which exhibit widely dispersed, broad signals that are essentially uninterpretable. The two hydrogens associated with cobalt centers in each species are assigned by analogy with well-characterized related complexes such as **4** (vide supra). The nickel-associated proton in **17** is, however, novel in carborane sandwich chemistry and its true location cannot be verified from the available data. In addition, it is entirely possible that either or both of these products are accompanied in solution by corresponding species bearing more or fewer metal-bound hydrogens; for example, a complex similar to **16** but having $Co^{III}H$ in place of Co^{IV} may well be present in small quantity, as is often observed in cobalt multidecker chemistry (e.g., see **2** and **3** above).

Scheme 5

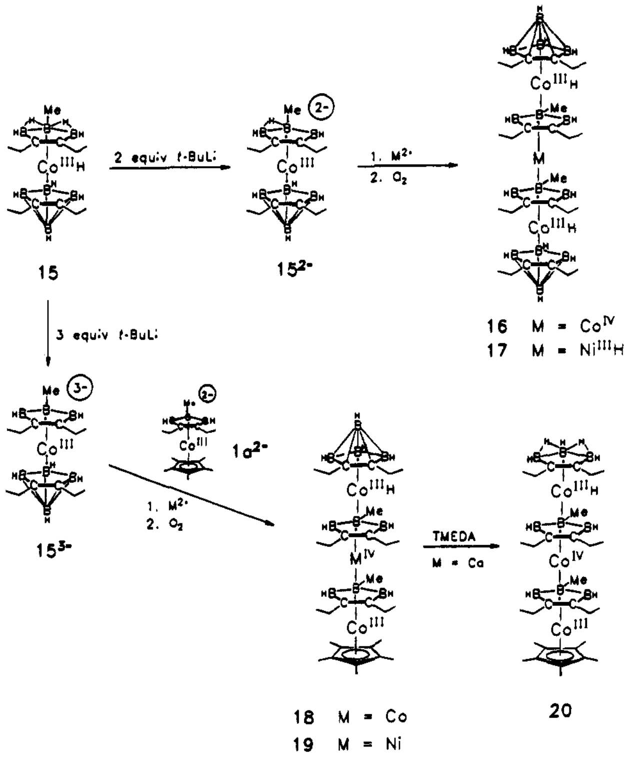

An attempt was made to decapitate the high-yield product **16**, since the expected decapped complex would be a potential synthon for building octadecker sandwiches via stacking with metal ions. However, reactions with TMEDA and with HCl/acetate gave fused products rather than the desired species. Nonetheless, it is likely that suitably functionalized derivatives of **16** and **17** can be decapitated, and efforts in this area are continuing.

The carborane-monocapped tetradeckers $(Et_2C_2B_4H_4)Co(Et_2C_2B_3H_2Me)M(Et_2C_2B_3H_2Me)CoCp^*$ (**18**, M = Co; **19**, M = Ni) were generated via mixed-ligand reactions involving the trianion $\mathbf{15}^{3-}$, the dianion $\mathbf{1a}^{2-}$, and cobaltous or nickelous ion, as depicted in Scheme 5. As expected, the formation of **18** and **19** was accompanied by competitive reactions that generated the "symmetrical" carborane-bicapped species **16** and **17** as side products; following workup in air, **18** and **19** were isolated as black solids of mass 706, in 46% and 16% yield, respectively. Complex **18**, like its carborane-bicapped counterpart **16**, is paramagnetic with 41 ve, but **19** is diamagnetic and is formulated as a Ni(IV) 42 ve species. The asymmetry of these sandwiches, whose four ring ligands are inequivalent, is reflected in the relatively complex NMR spectra of **19**. The ^1H NMR spectrum (Table 1) is informative: the three ethyl CH_3 triplet

---

(20) Maxwell, W. M.; Miller, V. R.; Grimes, R. N. *J. Am. Chem. Soc.* **1976**, *98*, 4818.

(21) Meng, X.; Waterworth, S.; Sabat, M.; Grimes, R. N. *Inorg. Chem.* **1993**, *32*, 3188.

(22) Piepgrass, K. W.; Meng, X.; Hölscher, M.; Sabat, M.; Grimes, R. N. *Inorg. Chem.* **1992**, *31*, 5202.

(23) See ref 18, Figure 3c.

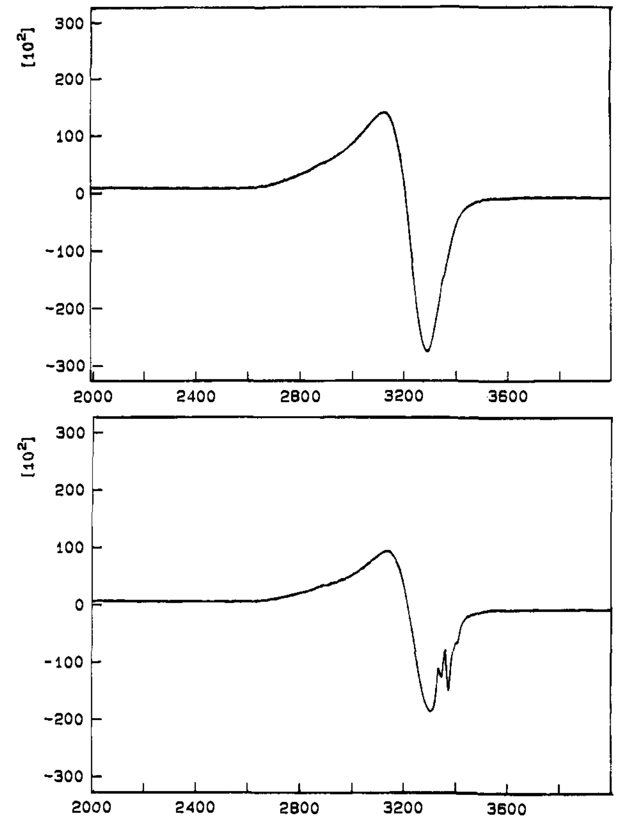

Figure 2. ESR spectra of **18** (top) and **20** (bottom).

resonances are apparent, as are several ethyl CH_2 multiplets and the broad high-field CoH proton resonance. One of the B-CH_3 signals appears as a singlet at δ 1.42 ppm, as expected, but curiously, the other is seen as a doublet at δ 1.53; since one of these B-methyl groups is close to the CoH group, the doublet signal may indicate coupling of B-CH_3 with that proton. The ^{11}B NMR spectrum of **19** also supports the proposed structure, with resonances observed for all seven boron environments.

The X-band ESR spectrum of paramagnetic **18** at 115 K is characteristic of axial symmetry, but the parallel and perpendicular regions are close and partially overlapped (Figure 2, top). No hyperfine structure is seen. Differences in the ESR spectrum of this 41 ve complex compared to those of several previously reported[1a,22] 41 ve tetradeckers, e.g., $[Cp^*Co^{III}(Et_2C_2B_3H_2X)]_2$-$Fe^{III}H$ (X = Me or Cl) and $[Cp^*Co^{III}(Et_2C_2B_3H_2Cl)]_2Co^{IV}$, are attributed to the higher symmetry of the latter three species, each of which has identical $Cp^*CoC_2B_3$ end units.

Decapitation with TMEDA was attempted on both complexes, leading to decomposition in the case of **19** but proceeding successfully with **18** to give the open-faced tetradecker **20** as a 41 ve paramagnetic black solid in 65% yield (Scheme 5). The ESR spectrum of **20**, shown in Figure 2 (bottom), is similar to that of **18** except that hyperfine splitting is observed, suggesting that the unpaired electron in **20** is relatively localized on the central cobalt atom. From a simple qualitative viewpoint, delocalization is expected to be more favored in **18**, whose carborane end cap creates a closo CoC_2B_4 cluster unit, than in **20**, which lacks this feature.

Electronic Absorption Spectra. The UV–visible spectra of the CoCo and NiCo triple-decker complexes **2–10** exhibit peak maxima that are redshifted by ca. 50 nm compared to their double-decker precursors, and the intensities are significantly and uniformly stronger in the triple-deckers. Thus, for **5** and **10** the extinction coefficients (in units of M^{-1} cm^{-1}) are 19 848 (λ_{max} = 336 nm) and 24 913 (λ_{max} = 372 nm), while those of **1a** and **1b** are 12 309 (λ_{max} = 284 nm) and 19 949 (λ_{max} = 286 nm) M^{-1} cm^{-1}, respectively. Although the magnitudes of these ϵ values are all within the normal range for charge-transfer excitations, the higher λ_{max} wavelengths in the triple-deckers, corresponding to lower-energy transitions, are consistent with more closely packed energy levels in the latter species.

The UV–visible spectra of the CoRu triple-deckers **12–14** are distinctly different from those of their CoCo and CoNi counterparts, the maxima of the former complexes appearing at shorter wavelengths; the extinction coefficients of the CoRu species are extremely high, e.g. that of **12** is 37 850 M^{-1} cm^{-1} at λ_{max} = 284 nm. As a second-row transition metal, ruthenum has higher-energy d levels than cobalt and nickel, which may contribute to a relatively higher antibonding e_1' LUMO[14] resulting in absorptions at shorter wavelengths than are observed in the CoCo and CoNi systems.

Concluding Remarks

Synthetic strategies that were employed earlier to prepare multidecker sandwiches capped by Cp, Cp*, or arene ligands have been applied in the present work to generate carborane-capped triple-deckers and tetradeckers that, in turn, open the way to higher-decker species. Several of these compounds have been utilized as precursors to penta- and hexadecker sandwiches, as we report in the following paper. Still larger stacks are anticipated, including possible hepta- and octadeckers that should be accessible via deprotonated anions generated from open-faced tetradecker complexes such as **20**. A particularly attractive class of target compounds would be "double open-ended" sandwiches containing C_2B_3 carborane rings on both ends, which would allow direct synthesis of polydecker systems via metal complexation. As we have previously noted, species of this type may eventually be accessible from C_2B_4-bicapped sandwiches such as **16** and **17** via decapitation at both ends.

Experimental Section

Instrumentation. ^{1}H NMR spectra (300 MHz) and ^{11}B NMR spectra (115.8 MHz) were recorded on GE QE-300 and Nicolet NT-360 spectrometers, respectively. Unit resolution mass spectra were obtained on a Finnegan MAT 4600 GC/MS spectrometer using perfluorotributylamine (FC43) as a calibration standard. In each case, a strong parent envelope was observed and the observed and calculated unit-resolution intensity patterns were in close agreement. Elemental analyses were conducted on a Perkin-Elmer 2400 CHN Analyzer using 2,4-dinitrophenylhydrazone as a standard. X-band ESR spectra were obtained at 115 K in CH_2Cl_2 glass on a Bruker ESP 300 spectrometer at 9.44 GHz. Visible–ultraviolet spectra were recorded on a Hewlett-Packard 8452A diode array with a HP Vectra computer interface.

Materials and Procedures. All reactions were conducted under an inert atmosphere unless otherwise indicated. Workup of products was generally carried out in air using benchtop procedures. Methylene chloride was distilled from CaH_2 and THF was distilled from Na/K alloy–benzophenone immediately prior to use. Column chromatography was performed on silica gel 60 (Merck) or neutral alumina. The starting complexes *nido*-$Cp^*Co(Et_2C_2B_3H_4$-5-Me) and *nido*-$Cp^*Co(Et_2C_2B_3H_2Me_3)$ were prepared as described elsewhere.[6a]

Synthesis of $Cp^*Co(Et_2C_2B_3H_2$-5-Me)$CoH(Et_2C_2B_4H_4)$ (2) and $Cp^*Co(Et_2C_2B_3H_2$-5-Me)$Co(Et_2C_2B_4H_4)$ (3). (a) From the $Cp^*Co(Et_2C_2B_3H_3$-5-Me)$^-$ and $Et_2C_2B_4H_5^-$ Monoanions. A previously described apparatus[23] consisting of a 3-neck flask (B) fitted with a rubber septum and a tip-tube and a second flask (A) having a septum and connected to flask B via a filter frit and a stopcock was charged with 74 mg (3.1 mmol) of NaH in flask A, 200 mg (0.61 mmol) of **1a** in flask B, and 79 mg (0.61 mmol) of dry $CoCl_2$ in the tip tube, and the entire apparatus was evacuated to high vacuum. THF (30 mL) was condensed into flask B at dry ice temperature (−78 °C), giving a yellow-orange solution which was isolated from the remainder of the apparatus by closing the stopcock. One equivalent of butyllithium in hexanes (0.25 mL of 2.5 M) was added to flask B at −78 °C via syringe, and the solution was warmed to room temperature and stirred for 30 min, producing a deep orange color. During this time, 30 mL of THF was condensed into flask A and 81 mg (0.61 mmol) of $(Et_2C_2B_4H_6)$ was added to A at −78 °C via syringe. Flask A was warmed to room temperature (during which time gas evolution was observed) and stirred for 30 min, after which the stopcock connecting flasks A and B was opened and the solution in A was transferred through the filter frit into B. The combined solution was cooled to −78 °C $CoCl_2$ was added from the tip tube, and the solution was warmed to room temperature during which it turned nearly black. The solution was stirred overnight and then opened to the air, and the solvent was removed by rotary evaporation leaving a black sludge. This material was washed through 2 cm of silica gel with hexane followed by CH_2Cl_2, affording 130 mg (0.40 mmol) of unreacted **1a** from the hexane fraction. The CH_2Cl_2 fraction was stripped of solvent, the dark brown residue was dissolved in a minimal volume of CH_2Cl_2/hexane, and this solution was placed on a silica gel column and eluted with 4:1 hexane−CH_2Cl_2. The first four bands, all minor, were discarded, followed by two major bands: brown **2** (39 mg, 0.076 mmol, 36% based on **1a** consumed), and dark brown **3** (35 mg, 0.068 mmol, 32%). MS base peaks (molecular ion envelopes, CI/CH_4): for **2**, *m/z* 515; for **3**, *m/z* 514. Anal. for **3**: Calcd for $Co_2C_{23}B_7H_{44}$, C 53.73, H 8.63; found C 53.56, H 8.58.

(b) From the $Cp^*Co(Et_2C_2B_3H_2\text{-}5\text{-}Me)^{2-}$ and $Et_2C_2B_4H_4{}^{2-}$ Dianions. The apparatus and procedure were similar to those employed in the monoanion reaction, except that 2 equiv of butyllithium were employed in order to generate the dianions; no NaH was used. Samples of 86 mg (0.65 mmol) of $Et_2C_2B_4H_6$, 213 mg (0.65 mmol) of **1a**, and 80 mg (0.65 mmol) of $CoCl_2$ were employed. After the reaction was set up as described above, the solution was stirred overnight, opened to the air, and the solvent was removed to give a black sludge which was worked up as before to give 75 mg (0.23 mmol) of recovered **1a** for the hexane fraction. The CH_2Cl_2 fraction was evaporated to dryness and eluted on a silica gel column in 4:1 hexane−CH_2Cl_2, which afforded several minor bands that were discarded, as well as two closely spaced major bands of **2** and **3** that moved very slowly in this solvent. The eluent was changed to 2:1 hexane−CH_2Cl_2 and then to a 1:1 mixture, which caused the two bands to merge. These were collected as a mixture of **2** and **3** (130 mg, 0.25 mmol, 60%), whose components were identical with the products of the monoanion-based synthesis, as shown from their NMR and mass spectra and TLC retention times. This mixture was conveniently used in the subsequent preparation of **4** (vide infra).

Synthesis of $Cp^*Co(Et_2C_2B_3H_2\text{-}5\text{-}Me)CoH(Et_2C_2B_3H_5)$ (4). Although this compound can be prepared from **2** or **3** separately, for our purposes it was more efficient to employ the mixture obtained in the previous synthesis. Accordingly, 130 mg of this material, prepared as described above, was treated with 8 mL of TMEDA and 3 drops of water under a flow of N_2, the flask was evacuated, and the solution was stirred for 3 h at room temperature. Volatiles were removed under vacuum in a Schlenk line, leaving a green-black sludge which was washed through 2 cm of silica with CH_2Cl_2. The solvent was removed by rotary evaporation and the residue was dissolved in hexane and eluted with hexane on a silica column. One major dark green band was obtained, following two minor bands which were discarded. Removal of solvent afforded 69 mg (0.14 mmol, 55%) of black solid **4**. MS base peak (molecular ion envelope, CI/CH_4), *m/z* 505. Anal. Calcd for $Co_2C_{23}B_6H_{46}$, C 54.67, H 9.18; found C 54.98, H 8.79.

Synthesis of $Cp^*Co(Et_2C_2B_3H_2\text{-}5\text{-}Me)Co(Et_2C_2B_3H_5)$ (5). A flask was charged with 600 mg (1.19 mmol) of **4** and 72 mg (3.0 mmol) of dry NaH. THF (60 mL) was condensed into the flask at −78 °C under vacuum. Gas evolution was observed as the flask was warmed to room temperature and stirred for 3 h. The system was opened to the air and solvent was removed, giving a dark brown solid which was column chromatographed as in the preceding synthesis, giving one dark brown band of **5** (500 mg, 0.99 mmol, 83%). MS base peak (molecular ion envelope, CI/CH_4), *m/z* 504. Anal. Calcd for $Co_2C_{23}B_6H_{45}$, C 54.78, H 8.99; found C 55.24, H 9.41.

Synthesis of $Cp^*Co(Et_2C_2B_3H_2\text{-}5\text{-}Me)CoH(Et_2C_2B_3H_4Br)$ (6). A flask was charged with 45 mg (0.090 mmol) of **4** and 30 mL of THF, and 1 equiv of *N*-bromosuccinimide was added via a tip-tube. The flask was warmed to room temperature and stirred overnight. The solvent was removed to give a black sludge which was washed through 2 cm of silica gel with CH_2Cl_2. The brown solution was evaporated to dryness and the residue was eluted in hexane on a silica gel column. The first band was unreacted **4**, 25 mg (0.05 mmol), and the second band was **6**, 9 mg (0.015 mmol, 38%). MS base peak (molecular ion envelope, CI/CH_4), *m/z* 584. Anal. Calcd for $BrCo_2C_{23}B_6H_{45}$, C 47.28, H 7.76; found C 47.30, H 8.17.

Synthesis of $Cp^*Co(Et_2C_2B_3H_2\text{-}5\text{-}Me)Co(Et_2C_2B_3H_4Br)$ (7) and $Cp^*Co(Et_2C_2B_3H_2\text{-}5\text{-}Me)Co(Et_2C_2B_3H_3Br_2)$ (8). The preceding procedure was followed employing 116 mg (0.23 mmol) of **5** and 1 equiv of *N*-bromosuccinimide (41 mg). Silica gel chromatography generated three dark brown bands, which were identified as **5** (27 mg), **7** (34 mg, 0.058 mmol, 33%), and **8** (32 mg, 0.048 mmol, 27%). MS base peaks (molecular ion envelopes, CI/CH_4): for **7**, *m/z* 583; for **8**, *m/z* 663. Anal. for **7**: Calcd for $BrCo_2C_{23}B_6H_{44}$, C 47.37, H 7.60; found C 47.38, H 7.96. Anal. for **8**: Calcd for $Br_2Co_2C_{23}B_6H_{43}$, C 41.72, H 6.55; found C 41.30, H 7.29.

Synthesis of $Cp^*Co(Et_2C_2B_3Me_3)Ni(Et_2C_2B_4H_4)$ (10). The setup and procedures described above for the preparation of **2** and **3** from the carborane and cobaltacarborane dianions were followed, using 2 equiv of butyllithium for the deprotonation of $Et_2C_2B_4H_6$ and **1b**. Samples of 225 mg (0.63 mmol) of **1b**, 83 mg (0.63 mmol) of $Et_2C_2B_4H_6$, and 140 mg (0.63 mmol) of $NiBr_2$ were employed. On workup as before, 140 mg (0.39 mmol) of **1b** was recovered from the hexane fraction, and 27 mg (0.050 mmol, 21%) of **10** was obtained as the only major band in the CH_2Cl_2 fraction during silica gel chromatography in 3:1 hexane−CH_2Cl_2. MS base peak (molecular ion envelope, CI/CH_4), *m/z* 542. Anal. Calcd for $NiCoC_{25}B_7H_{48}$, C 55.41, H 8.93; found C 54.34, H 9.00.

Synthesis of $(CHMe_2C_6H_4Me)Ru(Et_2C_2B_3H_2\text{-}5\text{-}Me)Co(Et_2C_2B_4H_4)$ (12). The method employed in the syntheses of **2**, **3**, and **10** from dianionic substrates was used, employing 230 mg (0.65 mmol) of $(CHMe_2C_6H_4Me)Ru(Et_2C_2B_3H_4Me)$ (**11**), 86 mg (0.65 mmol) of $Et_2C_2B_4H_6$, 84 mg (0.65 mmol) of $CoCl_2$, and 2 equiv of butyllithium. Workup on silica columns gave 145 mg (0.39 mmol) of unreacted **11** from the hexane fraction, isolated as a pale yellow band. The CH_2Cl_2 fraction was further chromatographed in 2:1 hexane−CH_2Cl_2, affording 72 mg (0.13 mmol. 50%) of deep green **12** as the only major band. MS base peak (molecular ion envelope, CI/CH_4), *m/z* 556. Anal. Calcd for $RuCoC_{23}B_7H_{43}$, C 49.75, H 7.81; found C 50.38, H 8.08.

Synthesis of $(CHMe_2C_6H_4Me)Ru(Et_2C_2B_3H_2\text{-}5\text{-}Me)CoH(Et_2C_2B_3H_5)$ (13). The decapitation procedure used to prepare **4** as described above was followed using 67 mg (0.12 mmol) of **12**. Chromatography was conducted in 5:1 hexane−CH_2Cl_2, which eluted 42 mg (0.077 mmol, 64%) of red-brown **13**. MS base peak (molecular ion envelope, CI/CH_4), *m/z* 547. Anal. Calcd for $RuCoC_{23}B_6H_{45}$, C 50.55, H 8.30; found C 50.56, H 8.77.

Synthesis of $(CHMe_2C_6H_4Me)Ru(Et_2C_2B_3H_2\text{-}5\text{-}Me)Co(Et_2C_2B_3H_5)$ (14). The method employed in the synthesis of **5** from **4** was followed using 50 mg (0.091 mmol) of **13**. Chromatography in 3:1 hexane−CH_2Cl_2 gave 33 mg (0.060 mmol, 66%) of dark green **14** as the only band. MS base peak (molecular ion envelope, CI/CH_4), *m/z* 546. Anal. Calcd for $RuCoC_{23}B_6H_{44}$, C 50.65, H 8.13; found C 49.03, H 8.55.

Improved Synthesis of $(Et_2C_2B_3H_4\text{-}5\text{-}Me)CoH(Et_2C_2B_4H_4)$ (15). In place of the route described earlier[21] for the preparation of **15** via methylation of the cobaltacarborane monoanion, higher yields of this compound were obtained in the present work by employing the dianion. A 1.413-g (4.57 mmol) sample of $(Et_2C_2B_3H_5)CoH(Et_2C_2B_4H_4)$[21] was placed in a 2-neck flask fitted with a septum and attached to a vacuum line. THF was condensed into the flask at −78 °C under vacuum, giving a yellow-orange solution. Via syringe, 2 equiv of *tert*-butyllithium in pentane (5.3 mL, 1.7 M) were added, and the solution was warmed to room temperature and stirred for 30 min, during which the color changed to deep orange-red. Methyl iodide (643 mg, 4.53 mmol) was added via syringe and the solution was stirred overnight at room temperature, after which it was opened to the air and the solvent was stripped off. The red sludge was washed through 2 cm of silica with acetone, and the wash was column-chromatographed on silica, using first hexane and then 4:1 hexane−acetone to give one red-orange band. Evaporation of solvent gave 910 mg (2.78 mmol, 61%) of **15** as a red oil.

Synthesis of $Co[(Et_2C_2B_3H_2\text{-}5\text{-}Me)Co(Et_2C_2B_4H_4)]_2$ (16). A 185-mg (0.57 mmol) sample of **15** was placed in a 3-neck flask equipped with a septum and attached to a vacuum line. $CoCl_2$ (37 mg, 0.28 mmol) was placed in a tip-tube and attached to the third neck. THF was condensed into the flask at −78 °C in vacuum, giving an orange solution. To this solution were added, via syringe, 2 equiv of *tert*-butyllithium in pentane (0.67 mL, 1.7 M) and the solution was warmed to room temperature and stirred for 30 min during which it acquired a deep orange-red color. The solution was cooled in dry ice/ethanol and the $CoCl_2$ was added from the tip-tube. On warming to room temperature, the color changed to nearly black. After being stirred for 5 h, the solution was opened to the air and solvent was removed to give a dark brown-black sludge which was washed through 2 cm of silica with acetone, giving a brown solution. The acetone was stripped off to give an almost black oily solid, which was dissolved in a minimal amount of acetone and placed on a silica gel column and eluted with 1:2 hexane−acetone. One major dark brown band appeared following a minor brown band, which was discarded. After removal of solvent, the major band afforded 140 mg (0.20 mmol, 70%) of **16**. MS base peaks (CI/CH_4): *m/z* 701 (molecular ion envelope), 324 $((Et_2C_2B_3H_4\text{-}Me)CoH(Et_2C_2B_4H_4)^+$ fragment). Anal. Calcd for $Co_3C_{26}B_{14}H_{60}$, C 44.55, H. 8.63; found C 45.76, H 8.70.

Synthesis of $NiH[(Et_2C_2B_3H_2\text{-}5\text{-}Me)Co(Et_2C_2B_4H_4)]_2$ (17). The procedure employed in the preceding synthesis was followed using 116 mg (0.36 mmol) of **15** and 39 mg (0.18 mmol) of $NiBr_2$ to produce 44 mg (0.063 mmol, 35%) of black **17**. MS base peaks (CI/CH_4): *m/z* 701 (molecular ion envelope), 324 $((Et_2C_2B_3H_4Me)CoH(Et_2C_2B_4H_4)^+$ fragment). Anal. Calcd for $NiCo_2C_{26}B_{14}H_{61}$, C 44.51, H 8.76; found C 45.43, H 9.44.

Synthesis of Cp*$Co(Et_2C_2B_3H_2\text{-}5\text{-}Me)Co(Et_2C_2B_3H_2\text{-}5\text{-}Me)CoH(Et_2C_2B_4H_4)$ (18). The experimental setup used in the preparation of **2** and **3** above, and described in an earlier publication,[23] was charged with 231 mg (0.70 mmol) of **1a** in flask B, 225 mg (0.70 mmol) of **15** in flask A, and 91 mg of $CoCl_2$ in the tip-tube. The apparatus was evacuated and THF was condensed into flask B at −78 °C, giving a yellow-orange solution which was isolated by closing the stopcock. After addition of 2 equiv of *tert*-butyllithium via syringe at −78 °C, the solution was warmed to room temperature and stirred for 30 min, producing a deep orange color. During this procedure, THF was condensed into flask A at −78 °C to give an orange solution to which 3 equiv of *tert*-butyllithium were added via syringe, and again the solution was warmed to room temperature and stirred for 30 min, acquiring a deep orange-red color. The stopcock was opened, allowing the solution in A to filter into B through the sintered frit. The combined solution was cooled to −78 °C and the $CoCl_2$ was tipped in. On warming to room temperature, the solution turned nearly black. After it was stirred overnight, the solution was opened to the air, solvent was removed, and the black sludge remaining was washed through 2 cm of silica with hexane, followed by 1:1 hexane−CH_2Cl_2 and finally by acetone. The hexane wash was column-chromatographed on silica in hexane, affording 90 mg (0.28 mmol) of unreacted **1a**. The hexane−CH_2Cl_2 wash was chromatographed using 2:1 hexane−CH_2Cl_2, giving a brown band (discarded) followed by a purple band of **18** (133 mg, 0.19 mmol, 46% based on **1a** consumed). Chromatography of the acetone wash in 1:2 hexane−acetone gave one dark brown band which proved to be **16** (36 mg, 0.051 mmol, 12%). MS for **18**: base peak (molecular ion envelope, CI/CH_4), *m/z* 706. Anal. for **18**: Calcd for $Co_3C_{30}B_{10}H_{60}$, C 51.06, H 8.57; found C 51.01, H 8.73.

Synthesis of Cp*$Co(Et_2C_2B_3H_2\text{-}5\text{-}Me)Ni(Et_2C_2B_3H_2\text{-}5\text{-}Me)CoH(Et_2C_2B_4H_4)$ (19). The operations described in the preceding synthesis were followed using 102 mg (0.31 mmol) of **15**, 104 mg (0.31 mmol) of **1a**, and 72 mg (0.33 mmol) of $NiBr_2$. Chromatography as above gave 20 mg (0.062 mmol) of unreacted **1a**, 29 mg (0.041 mmol, 16%) of **19**, and a small quantity of **17**. MS for **19**: base peak (molecular ion envelope, CI/CH_4), *m/z* 706. Anal. for **19**: Calcd for $NiCo_2C_{30}B_{10}H_{60}$, C 51.08, H 8.57; found C 52.13, H 9.48.

Synthesis of Cp*$Co(Et_2C_2B_3H_2\text{-}5\text{-}Me)Co(Et_2C_2B_3H_2\text{-}5\text{-}Me)CoH(Et_2C_2B_3H_5)$ (20). An 80-mg (0.11 mmol) sample of **18** was placed in a 2-neck flask and 10 mL of TMEDA and 3 drops of water were added under a nitrogen flow. The situation was evacuated and the solution was stirred for 3 h at room temperature. The volatiles were removed under vacuum on a Schlenk line, and the black-brown residue was washed through 2 cm of silica with CH_2Cl_2. After removal of solvent, the dark brown solid was dissolved in hexane and CH_2Cl_2, placed on silica plates, and eluted with 2:1 hexane−CH_2Cl_2 to give two minor bands, which were discarded, and a major dark brown band which was **20** (50 mg, 0.072 mmol, 65%). Anal. Calcd for $Co_3C_{30}B_9H_{61}$, C 51.78, H 8.84; found C 51.70, H 8.88.

X-ray Structure Determination on 4. Diffraction data were collected on a Rigaku AFC6S diffractometer at −120 °C using Mo Kα radiation. Details of the data collection and structure determination are listed in Table 4. The unit cell dimensions were determined by least-squares refinement of the setting angles of 25 high-angle reflections. The intensities of three standard reflections, monitored at 3-h intervals, showed no significant variation. Empirical absorption corrections were applied following s scanning of several reflections (transmission factors are reported in Table 4). All calculations were performed on a VAX station 3520 computer employing the TEXSAN 5.0 crystallographic software package.[24] The structure was solved by direct methods in SIR88,[25] and full-matrix least-squares refinement with anisotropic thermal displacement parameters was carried out for all non-hydrogen atoms, with the results summarized in Table 4. All hydrogen atoms were located from difference Fourier maps. The carborane ring hydrogens were refined with isotropic thermal displacement parameters, and the remaining methyl and methylene hydrogens were included in the calculations without further refinement. The final difference Fourier map was featureless.

Acknowledgment. This work was supported by the U.S. Army Research Office and the National Science Foundation, Grant No. CHE 9322490. We wish to note the contributions of our late colleague Dr. Simon Waterworth, who was instrumental in developing the syntheses of **2** and **3**.[9] We thank Mr. Zhihai Qin and Dr. Yaning Wang of this department for obtaining the ESR spectra and for valuable discussions on those data.

Supporting Information Available: Tables of atomic coordinates (including hydrogen atom positions), anisotropic thermal parameters, and calculated mean planes for **4** (4 pages). This material is contained in many libraries on microfiche, immediately follows this article in the microfilm version of the journal, can be ordered from the ACS, and can be downloaded from the Internet; see any current masthead page for ordering information and Internet access instructions.

JA952741J

---

[24] TEXSAN 5.0: Single Crystal Structure Analysis Software (1989), Molecular Structure Corporation, The Woodlands, TX 77381.

[25] SIR88: Burla, M. C.; Camalli, M.; Cascarano, G.; Giacovazzo, C.; Polidori, G.; Spagna, R.; Viterbo, D. *J. Appl. Crystallogr.* **1989**, *22*, 389.